

Implications on the origin of cosmic rays in light of 10 TV spectral softenings

Chuan Yue^a, Peng-Xiong Ma^{a,b}, Qiang Yuan^{a,b,c*}, Yi-Zhong Fan^{a,b†}, Zhan-Fang Chen^{a,b}, Ming-Yang Cui^a, Hao-Ting Dai^d, Tie-Kuang Dong^a, Xiaoyuan Huang^a, Wei Jiang^{a,b}, Shi-Jun Lei^a, Xiang Li^a, Cheng-Ming Liu^d, Hao Liu^a, Yang Liu^a, Chuan-Ning Luo^{a,b}, Xu Pan^{a,b}, Wen-Xi Peng^e, Rui Qiao^e, Yi-Feng Wei^d, Li-Bo Wu^d, Zhi-Hui Xu^{a,b}, Zun-Lei Xu^a, Guan-Wen Yuan^{a,b}, Jing-Jing Zang^a, Ya-Peng Zhang^f, Yong-Jie Zhang^f, and Yun-Long Zhang^d

^aKey Laboratory of Dark Matter and Space Astronomy,

Purple Mountain Observatory, Chinese Academy of Sciences, Nanjing 210033, China

^bSchool of Astronomy and Space Science, University of Science and Technology of China, Hefei 230026, China

^cCenter for High Energy Physics, Peking University, Beijing 100871, China

^dState Key Laboratory of Particle Detection and Electronics,

University of Science and Technology of China, Hefei 230026, China

^eKey Laboratory of Particle Astrophysics, Institute of High Energy Physics, Chinese Academy of Sciences, Beijing 100049, China

^fInstitute of Modern Physics, Chinese Academy of Sciences, Lanzhou 730000, China

(Dated: December 3, 2019)

Precise measurements of the energy spectra of cosmic rays (CRs) show various kinds of features deviating from single power-laws, which give very interesting and important implications on their origin and propagation. Previous measurements from a few balloon and space experiments indicate the existence of spectral softenings around 10 TV for protons (and probably also for Helium nuclei). Very recently, the DARK MATTER PARTICLE EXPLORER (DAMPE) measurement about the proton spectrum clearly reveals such a softening with a high significance. Here we study the implications of these new measurements, as well as the groundbased indirect measurements, on the origin of CRs. We find that a single component of CRs fails to fit the spectral softening and the air shower experiment data simultaneously. In the framework of multiple components, we discuss two possible scenarios, the multiple source population scenario and the background plus nearby source scenario. Both scenarios give reasonable fits to the wide-band data from TeV to 100 PeV energies. Considering the anisotropy observations, the nearby source model is favored.

PACS numbers: 96.50.S-

I. INTRODUCTION

The origin of cosmic rays (CRs) remains an unresolved question after more than one century since their discovery. To identify the sources of CRs is difficult due to that the diffusive propagation of charged particles in the random magnetic field results in the loss of the original directions of CRs. Precise measurements of the energy spectra of various species of CRs are helpful in understanding their origin and propagation. The energy spectra of CRs from the acceleration sources are generally believed to be power-laws with cutoffs due to the maximum acceleration limits of specific types of sources. The diffusion in the Galaxy results in softenings of the accelerated spectra, by a power-law of $E^{-\delta}$, which reflects the energy-dependence of the diffusion coefficient and hence the turbulent properties of the interstellar medium. Such an effect has been supported by the measurement of the secondary-to-primary flux ratios of CR nuclei [1].

However, several balloon and space experiments revealed remarkable spectral hardenings of CR nuclei around a few hundred GV rigidities [2–8]. These results inspire quite a number of discussions of their possible implications on the origin [9–15], acceleration [16–18], and propagation [19–26] of CRs. The AMS-02 measurements of the spectra of the secondary family of nuclei, Li, Be, and B, show that on aver-

age their spectra harden above ~ 200 GV by $E^{0.13}$ more than that of the primary family of He, C, and O [27], which indicates that the spectral hardenings may have a propagation origin [28]. Nevertheless, it is shown that the injection hardening scenario can also fit the data reasonably well in a class of propagation models with effective reacceleration of particles in the turbulent medium [29, 30].

Improved direct measurements of the CR spectra at higher energies are recently available from several experiments. Interestingly, the CREAM [31] and NUCLEON [32] data show hints that the CR spectra become softer for rigidities higher than 10 TV. The precise measurement of the proton spectrum up to 100 TeV by the Dark Matter Particle Explorer (DAMPE; [33, 34]) clearly reveal such a spectral softening [35]. On the other hand, ground-based air shower experiments show that the all-particle spectrum has a so-called “knee” at energies of a few PeV (e.g., [36–39]). Measurements of the knee of individual composition have relatively large uncertainties [36, 40]. A few measurements of the light composition group, e.g. proton plus helium nuclei, tend to suggest a knee below PeV energies [41]. Most recently, preliminary results about the proton plus helium spectra measured by the HAWC experiment showed also a softening at about 30 TeV energies [42]. Given all these progresses of the measurements, it is thus very interesting to investigate the implications of the wide-band direct and indirect measurements on the CR modeling.

There are some studies based on the data available at different time [45–51]. In particular, several studies propose to account for various spectral structures using multiple populations of CR sources [46–49]. Alternatively, if there are by

*Corresponding author: yuanq@pmo.ac.cn

†Corresponding author: yzf@pmo.ac.cn

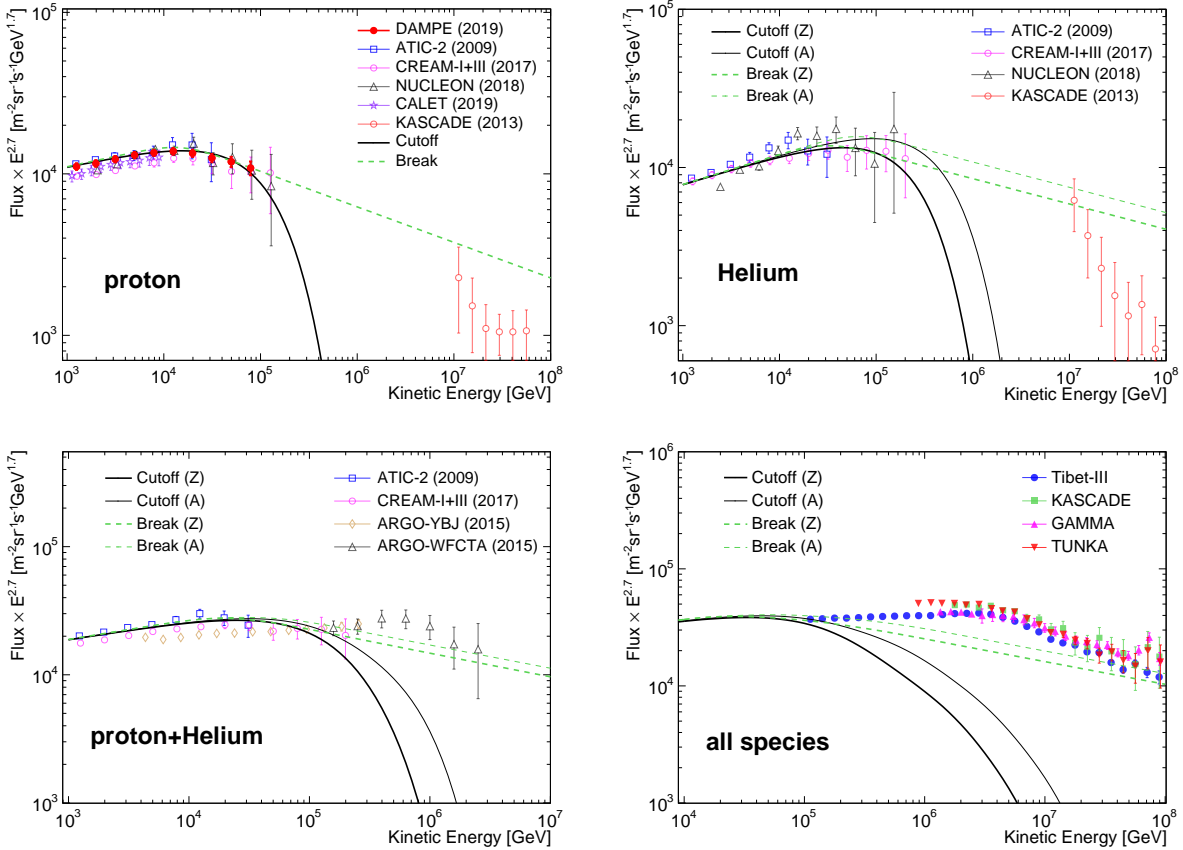


FIG. 1: Energy spectra of protons (top-left), Helium (top-right), proton plus Helium (bottom-left), and all species (bottom-right). In each panel the solid lines show the fitting results with an exponential cutoff form (eq.(1)), and the dashed lines show the broken power-law (eq.(2)) fitting results. The thick lines are for the Z -dependent cutoff/break energies, and the thin lines are for the A -dependent cases. References of the data: protons, ATIC [2], CREAM [31], NUCLEON [32], CALET [8], DAMPE [35], KASCADE [43]; Helium, ATIC [2], CREAM [31], NUCLEON [32], KASCADE [43]; $p+He$, ATIC [2], CREAM [31], ARGO-YBJ [44], ARGO-WFCTA [41]; all-particle, Tibet-III [38], KASCADE [36], GAMMA [39], TUNKA [37].

chance one or a few nearby sources whose contributions are different from the sum of the other background sources, spectral structures may also be produced [52–58]. In light of the new measurements of the CR spectra, in particular, by the DAMPE, we revisit the modeling of CR sources from TeV to 100 PeV in a phenomenological way. Our discussion is within the framework of the above two scenarios, i.e. multiple populations (denoted as model A) and nearby sources (denoted as model B), but with a focus on the $O(10)$ TV spectral features. Both models have good physical motivations. For model A, for example, the remnants of different types of supernovae which are smoothly distributed in the Galactic disk should behave differently in accelerating CR particles. The sum of their contributions can result in complicated spectral features. Alternatively, if the Earth is close to (e.g., $\lesssim 500$ pc) one single accelerator by chance, the distinct spectral feature from this nearby source may naturally give the observed spectral bumps. The purpose of this study is to build an overall model of CRs to describe as many as possible the up-to-date observational data in a wide energy range.

II. ORIGIN OF THE SPECTRAL SOFTENING

It is clear that the spectral softening around ~ 10 TV do not correspond to the PeV knee of CRs, even for A -dependent knees of various compositions. To see this explicitly, we show in Fig. 1 the energy spectra of protons, Helium, protons plus Helium, and the all-particle one, for the fitting with one single component of each species. We assume either an exponential cutoff power-law form or a broken power-law form to describe the spectral softening of CR nuclei, as

$$\Phi_i(E) = \Phi_{0,i} \left(\frac{E}{\text{TeV}} \right)^{-\gamma_i} \times \exp\left(-\frac{E}{E_{c,i}}\right), \quad (1)$$

and

$$\Phi_i(E) = \Phi_{0,i} \left(\frac{E}{\text{TeV}} \right)^{-\gamma_i} \times \left[1 + \left(\frac{E}{E_{b,i}} \right)^s \right]^{(-\Delta\gamma/s)}, \quad (2)$$

where E is the total energy of a particle, the subscription i represents different nuclear species, γ_i is the spectral index

below the energy of the softening, $E_{b,i}$ ($E_{c,i}$) is the break (cutoff) energy, s is a smoothness parameter, and $\Delta\gamma$ is the change of the spectral index above $E_{b,i}$. These parameters are determined through fitting to the measurements of energy spectra of individual species by ATIC [2], CREAM [31, 59], NUCLEON [32], and DAMPE [35]. For different nuclear species, we assume that the break (cutoff) energy $E_{b,i}$ ($E_{c,i}$) is proportional to either the atomic number Z_i or the mass number A_i , i.e., $E_{b,i} = Z_i\epsilon_b$ or $A_i\epsilon_b$ ($E_{c,i} = Z_i\epsilon_c$ or $A_i\epsilon_c$). For the broken power-law fit, the proton spectrum suggests that $s = 3.0$ and $\Delta\gamma = 0.35$ can describe the spectral softening well. The other parameters are given in Table I. The results show that the p+He and the all-particle spectra cannot be reproduced in all these fittings, and additional spectral structures between the $O(10)$ TV softening and the knee of CRs are expected (see also Ref. [60]). In the following we discuss two natural scenarios of these spectral structures.

A. Multiple populations of CR sources

It has been widely postulated that there are more than one populations of CR sources in the Milky Way. For instance, supernovae of different types may accelerate particles to different maximum energies, giving various spectral features of CRs [46, 49]. Following Ref. [49], we assume that the spectrum of each population is described by an exponential cutoff power-law function of eq. (1). We further assume that the cutoff energies of different species of each population depend on the atomic number Z_i , i.e., $E_{c,i} = Z_i\epsilon_c$. The fitting results of the major species as well as the all-particle spectrum are shown in Fig. 2. The spectral parameters are summarized in Table II.

In this scenario, the spectral bumps around 10 TeV are ascribed to the cutoff of population I, with a characteristic cutoff rigidity of ~ 60 TV. The spectra become harder again for rigidities higher than ~ 100 TV, due to the contribution from population II. The cutoff rigidity of population II is about 4 PV, which corresponds to the knee of the all-particle spectrum. We note that the expected spectrum of p+He of this model should also show bump-like feature as that seen in the spectra of protons and Helium. The data from CREAM do show hints of this kind of feature [31]. The preliminary result about the p+He spectrum by HAWC also shows the bump feature at ~ 30 TeV [42], consistent with the model fittings in this work. However, the ARGO-WFCTA data show that the knee of the p+He spectrum is around 700 TeV, which is lower than the $4 \sim 8$ PeV obtained in our fittings. This is because we use the KASCADE measurements to determine the cutoff energy of population II. As shown in Ref. [51], the fitting to KASCADE data does favor a higher cutoff energy than the fitting to ARGO data. Improved measurements of the p+He spectra above 100 TeV energies are necessary to understand this slight tension.

B. Nearby source(s)

The other scenario to ascribe these spectral features to the contribution of nearby source(s). We assume that the majorities of the observed CR fluxes are due to a background component from the population of sources, and a nearby source component contributes to the ~ 10 TV spectral bumps. The energy spectra of both the background and the nearby components are assumed to be exponentially cutoff power-law functions. The fitting results are shown in Fig. 3, with best-fit parameters compiled in Table III. For the nearby source, the spectral index is about 2.1 and the cutoff rigidity is about 20 TV. Note that in Ref. [55] a slightly higher cutoff rigidity of ~ 70 TV was derived to fit the CREAM data. This difference is probably due to that the DAMPE data is used in the fit here, and we neglect the CR propagation in this work. This nearby source model (model B) gives comparable goodness-of-fit to the current data, compared with model A described in Sec. III A. These two models may have slight differences in predicting the spectra between 100 TeV and 10 PeV where measurements are lacking. However, we should note that such differences may become smaller through adjusting the model parameters.

Nevertheless, there is a potentially significant difference between models A and B, i.e., the predicted anisotropy pattern of arrival directions of CRs. For model A, the predicted large-scale anisotropies of CRs are the same as the conventional CR diffusion model with a single component of source distribution. The amplitudes of the dipole anisotropies are proportional to E^δ , where δ is the energy-dependent slope of the diffusion coefficient. The direction of the anisotropy pattern points from the Galactic center to the anti-center. These model predictions are, however, inconsistent with the measurements of the anisotropies [62–66]. Model B can explain the anisotropy data well [54, 55]. As suggested in Ref. [55], a local source located in the direction that close to Geminga, together with the background source component, can simultaneously explain the spectral features of CR protons and Helium nuclei and the amplitudes and phases of the dipole anisotropies. Specifically, the nearby source dominates the low-energy ($E < 100$ TeV) anisotropies with phases being determined by the direction of the source, and the background dominates the high-energy ($E > 100$ TeV) anisotropies with phases pointing from the Galactic center to the anti-center.

III. CONCLUSION

Direct measurements of the CR spectra up to 100 TeV by CREAM, NUCLEON, and particularly by DAMPE with high-precision, reveal spectral softenings around ~ 10 TV rigidities. In this work we discuss possible origins of these results, taking into account the wide-band measurements of the CR energy spectra of various mass groups. We show that employing two populations of CR sources with cutoff rigidities of ~ 60 TV and ~ 4 PV can properly fit the measured energy spectra of the main species as well as the all-particle spectrum. Alternatively, including a nearby source on top of the back-

TABLE I: Spectral parameters of major CR species assuming ~ 10 TV knees.

Species	$\Phi_{0,i}$ ($\text{m}^{-2}\text{s}^{-1}\text{sr}^{-1}\text{TeV}^{-1}$)	γ_i	ϵ_b (TeV)	ϵ_c (TeV)
p	8.79×10^{-2}	2.57	15	120
He	6.20×10^{-2}	2.51	15	120
C	1.05×10^{-2}	2.56	15	120
O	1.35×10^{-2}	2.56	15	120
Ne	4.73×10^{-3}	2.56	15	120
Mg	7.43×10^{-3}	2.56	15	120
Si	8.78×10^{-3}	2.56	15	120
Fe	1.50×10^{-2}	2.56	15	120

TABLE II: Spectral parameters of model A.

Species	Pop. I			Pop. II		
	$\Phi_{0,i}$ ($\text{m}^{-2}\text{s}^{-1}\text{sr}^{-1}\text{TeV}^{-1}$)	γ_i	ϵ_c (TeV)	$\Phi_{0,i}$ ($\text{m}^{-2}\text{s}^{-1}\text{sr}^{-1}\text{TeV}^{-1}$)	γ_i	ϵ_c (TeV)
p	7.78×10^{-2}	2.60	56	1.15×10^{-2}	2.33	4.0×10^3
He	5.84×10^{-2}	2.51	56	6.30×10^{-3}	2.30	4.0×10^3
C	9.92×10^{-3}	2.50	56	7.00×10^{-4}	2.30	4.0×10^3
O	1.66×10^{-2}	2.50	56	1.10×10^{-3}	2.30	4.0×10^3
Ne	2.40×10^{-3}	2.50	56	1.37×10^{-4}	2.30	4.0×10^3
Mg	3.52×10^{-3}	2.50	56	2.22×10^{-4}	2.30	4.0×10^3
Si	6.08×10^{-3}	2.50	56	3.71×10^{-4}	2.30	4.0×10^3
Fe	7.78×10^{-3}	2.37	56	2.27×10^{-3}	2.30	4.0×10^3

TABLE III: Spectral parameters of model B.

Species	Background			Nearby source		
	$\Phi_{0,i}$ ($\text{m}^{-2}\text{s}^{-1}\text{sr}^{-1}\text{TeV}^{-1}$)	γ_i	ϵ_c (TeV)	$\Phi_{0,i}$ ($\text{m}^{-2}\text{s}^{-1}\text{sr}^{-1}\text{TeV}^{-1}$)	γ_i	ϵ_c (TeV)
p	7.41×10^{-2}	2.66	6.0×10^3	1.18×10^{-2}	2.10	18
He	5.55×10^{-2}	2.60	6.0×10^3	9.30×10^{-3}	2.10	18
C	1.02×10^{-2}	2.60	6.0×10^3	1.10×10^{-3}	2.10	18
O	1.63×10^{-2}	2.60	6.0×10^3	2.20×10^{-3}	2.10	18
Ne	2.40×10^{-3}	2.60	6.0×10^3	2.64×10^{-4}	2.10	18
Mg	3.52×10^{-3}	2.60	6.0×10^3	4.03×10^{-4}	2.10	18
Si	6.08×10^{-3}	2.60	6.0×10^3	6.37×10^{-4}	2.10	18
Fe	1.16×10^{-2}	2.48	6.0×10^3	1.28×10^{-3}	2.10	18

ground component gives similar fitting to the spectra. The nearby source model can additionally explain the amplitudes and phases of the large-scale anisotropies of CRs, as long as the source is located at a proper direction in the sky. It has been found that the Geminga supernova remnant may be a promising candidate of such a local source [55].

The revealing of new spectral features of CRs is shown to be able to give very interesting implications on the physics of CRs. The measurement uncertainties of the energy spectra of different mass groups are relatively large for energies

higher than 100 TeV, due to the low statistics (for space detection) or the poor composition resolution (for ground-based detection). The under construction Large High Altitude Air Shower Observatory (LHAASO; [67]) and the proposed High Energy cosmic-Radiation Detection (HERD; [68]) facility onboard the Chinese Space Station are expected to significantly improve the precision of CR spectral measurements. Particularly, the measurements of anisotropies of different mass groups by LHAASO will be essentially helpful in understanding the spectral softening features, the knee structures, and the

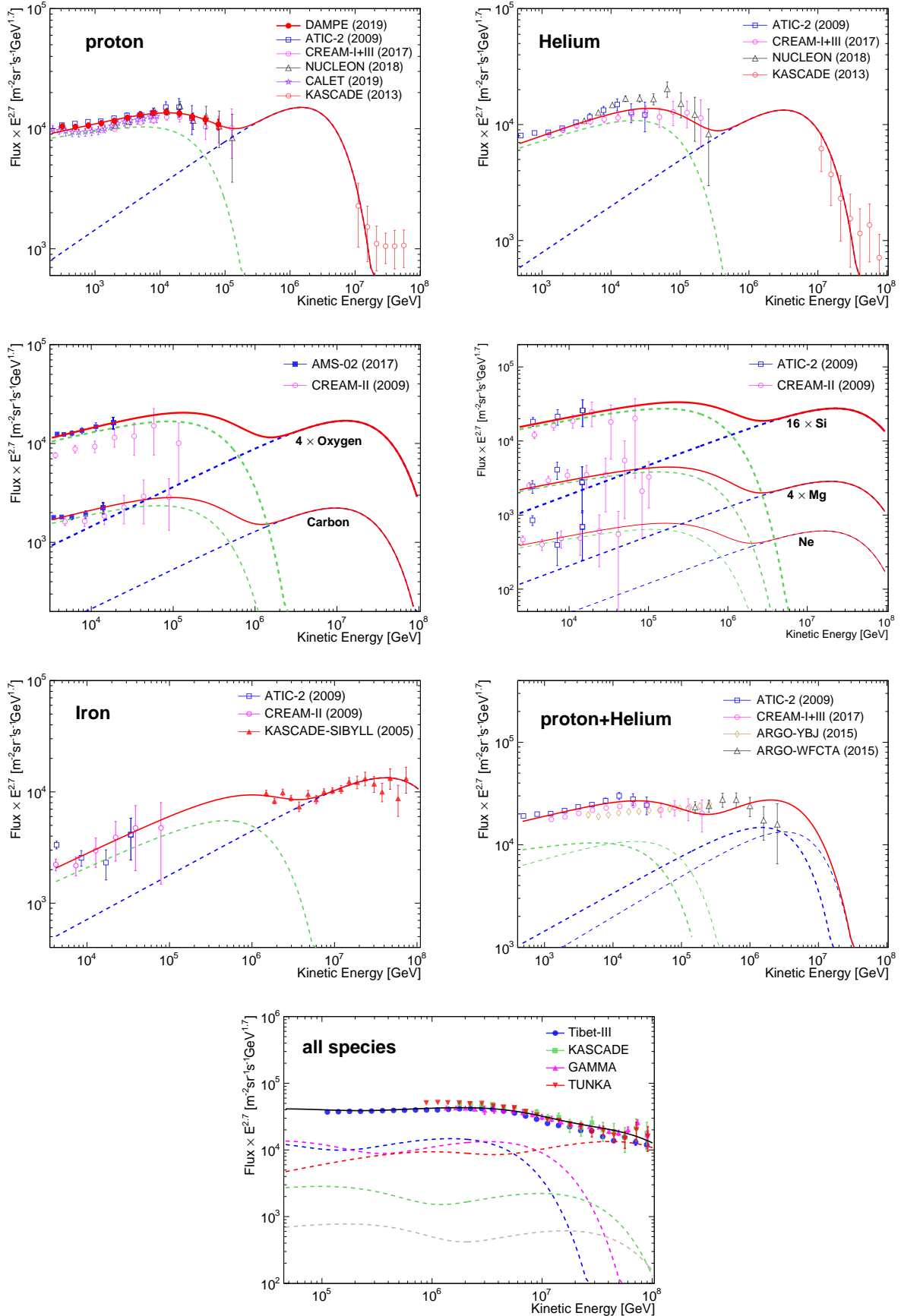


FIG. 2: Fitting energy spectra for model A, compared with the data. In each panel, the green and blue dashed curves show the contributions of each source population, and the solid curves are the total contribution. References of the data: Carbon and Oxygen, AMS-02 [7], CREAM [61]; Neon, Magnesium, and Silicon, ATIC [2], CREAM [61]; Iron, ATIC [2], CREAM [61], KASCADE [36]. The other references are the same as in Fig. 1.

origin of CRs in general.

Acknowledgments

This work is supported by the National Key Research and Development Program of China (No. 2016YFA0400200),

the National Natural Science Foundation of China (Nos. 11722328, 11525313, U1738205, 11851305), and the 100 Talents Program of Chinese Academy of Sciences.

-
- [1] M. Aguilar, et al., *Phys. Rev. Lett.* **117**, 231102 (2016).
- [2] A. D. Panov, et al., *Bulletin of the Russian Academy of Science, Phys.* **73**, 564 (2009), 1101.3246.
- [3] H. S. Ahn, et al., *Astrophys. J. Lett.* **714**, L89 (2010), 1004.1123.
- [4] O. Adriani, et al., *Science* **332**, 69 (2011), 1103.4055.
- [5] M. Aguilar, et al., *Phys. Rev. Lett.* **114**, 171103 (2015).
- [6] M. Aguilar, et al., *Phys. Rev. Lett.* **115**, 211101 (2015).
- [7] M. Aguilar, et al., *Phys. Rev. Lett.* **119**, 251101 (2017).
- [8] O. Adriani, et al., *Phys. Rev. Lett.* **122**, 181102 (2019), 1905.04229.
- [9] Y. Ohira and K. Ioka, *Astrophys. J. Lett.* **729**, L13 (2011), 1011.4405.
- [10] Q. Yuan, B. Zhang, and X.-J. Bi, *Phys. Rev. D* **84**, 043002 (2011), 1104.3357.
- [11] A. E. Vladimirov, G. Jóhannesson, I. V. Moskalenko, and T. A. Porter, *Astrophys. J.* **752**, 68 (2012), 1108.1023.
- [12] A. D. Erlykin and A. W. Wolfendale, *Astroparticle Physics* **35**, 449 (2012).
- [13] S. Thoudam and J. R. Hörandel, *Mon. Not. Roy. Astron. Soc.* **421**, 1209 (2012), 1112.3020.
- [14] G. Bernard, T. Delahaye, Y.-Y. Keum, W. Liu, P. Salati, and R. Taillet, *Astron. Astrophys.* **555**, A48 (2013), 1207.4670.
- [15] W. Liu, X.-J. Bi, S.-J. Lin, B.-B. Wang, and P.-F. Yin, *Phys. Rev. D* **96**, 023006 (2017), 1611.09118.
- [16] V. Ptuskin, V. Zirakashvili, and E.-S. Seo, *Astrophys. J.* **763**, 47 (2013), 1212.0381.
- [17] S. Thoudam and J. R. Hörandel, *Astron. Astrophys.* **567**, A33 (2014), 1404.3630.
- [18] Y. Zhang, S. Liu, and Q. Yuan, *Astrophys. J. Lett.* **844**, L3 (2017), 1707.00262.
- [19] N. Tomassetti, *Astrophys. J. Lett.* **752**, L13 (2012), 1204.4492.
- [20] P. Blasi, E. Amato, and P. D. Serpico, *Phys. Rev. Lett.* **109**, 061101 (2012), 1207.3706.
- [21] N. Tomassetti and F. Donato, *Astrophys. J. Lett.* **803**, L15 (2015), 1502.06150.
- [22] A. M. Taylor and G. Giacinti, *Phys. Rev. D* **95**, 023001 (2017), 1607.08862.
- [23] C. Jin, Y.-Q. Guo, and H.-B. Hu, *Chinese Physics C* **40**, 015101 (2016), 1504.06903.
- [24] Y.-Q. Guo, Z. Tian, and C. Jin, *Astrophys. J.* **819**, 54 (2016).
- [25] Y.-Q. Guo and Q. Yuan, *Phys. Rev. D* **97**, 063008 (2018), 1801.05904.
- [26] W. Liu, Y.-h. Yao, and Y.-Q. Guo, *Astrophys. J.* **869**, 176 (2018), 1802.03602.
- [27] M. Aguilar, et al., *Phys. Rev. Lett.* **120**, 021101 (2018).
- [28] Y. Génolini, et al., *Phys. Rev. Lett.* **119**, 241101 (2017), 1706.09812.
- [29] Q. Yuan, C.-R. Zhu, X.-J. Bi, and D.-M. Wei, *arXiv e-prints* (2018), 1810.03141.
- [30] J.-S. Niu, T. Li, and H.-F. Xue, *arXiv e-prints* (2018), 1810.09301.
- [31] Y. S. Yoon, et al., *Astrophys. J.* **839**, 5 (2017), 1704.02512.
- [32] E. Atkin, et al., *Soviet Journal of Experimental and Theoretical Physics Letters* **108**, 5 (2018), 1805.07119.
- [33] J. Chang, *Chinese Journal of Space Science* **34**, 550 (2014).
- [34] J. Chang, et al., *Astroparticle Physics* **95**, 6 (2017), 1706.08453.
- [35] Q. An, et al., *Science Advances* **5**, eaax3793 (2019), 1909.12860.
- [36] T. Antoni, et al., *Astropart. Phys.* **24**, 1 (2005), astro-ph/0505413.
- [37] E. E. Korosteleva, V. V. Prosin, L. A. Kuzmichev, and G. Navarra, *Nuclear Physics B Proceedings Supplements* **165**, 74 (2007).
- [38] M. Amenomori, et al., *Astrophys. J.* **678**, 1165 (2008), 0801.1803.
- [39] A. P. Garyaka, R. M. Martirosov, S. V. Ter-Antonyan, A. D. Erlykin, N. M. Nikolskaya, Y. A. Gallant, L. W. Jones, and J. Procureur, *Journal of Physics G Nuclear Physics* **35**, 115201 (2008), 0808.1421.
- [40] Tibet Asy Collaboration, et al., *Physics Letters B* **632**, 58 (2006), astro-ph/0511469.
- [41] B. Bartoli, et al., *Phys. Rev. D* **92**, 092005 (2015), 1502.03164.
- [42] J. C. Arteaga-Velazquez and J. D. Alvarez, *Proceedings of Science ICRC2019*, 176 (2019).
- [43] W. D. Apel, et al., *Astroparticle Physics* **47**, 54 (2013).
- [44] B. Bartoli, et al., *Phys. Rev. D* **91**, 112017 (2015), 1503.07136.
- [45] J. R. Hörandel, *Astropart. Phys.* **19**, 193 (2003), astro-ph/0210453.
- [46] V. I. Zatsepin and N. V. Sokolskaya, *Astron. Astrophys.* **458**, 1 (2006), astro-ph/0601475.
- [47] A. M. Hillas, *arXiv Astrophysics e-prints* (2006), astro-ph/0607109.
- [48] T. K. Gaisser, *Astroparticle Physics* **35**, 801 (2012), 1111.6675.
- [49] T. K. Gaisser, T. Stanev, and S. Tilav, *Frontiers of Physics* **8**, 748 (2013), 1303.3565.
- [50] S. Thoudam, J. P. Rachen, A. van Vliet, A. Achterberg, S. Buitink, H. Falcke, and J. R. Hörandel, *Astron. Astrophys.* **595**, A33 (2016), 1605.03111.
- [51] Y.-Q. Guo and Q. Yuan, *Chinese Physics C* **42**, 075103 (2018), 1701.07136.
- [52] A. D. Erlykin and A. W. Wolfendale, *J. Phys. G Nucl. Phys.* **23**, 979 (1997).
- [53] L. G. Sveshnikova, O. N. Strelnikova, and V. S. Ptuskin, *Astroparticle Physics* **50**, 33 (2013), 1301.2028.
- [54] V. Savchenko, M. Kachelrieß, and D. V. Semikoz, *Astrophys. J. Lett.* **809**, L23 (2015), 1505.02720.
- [55] W. Liu, Y.-Q. Guo, and Q. Yuan, *J. Cosmol. Astropart. Phys.* **10**, 010 (2019), 1812.09673.
- [56] X. Qu, *arXiv e-prints* (2019), 1901.00249.
- [57] B.-Q. Qiao, W. Liu, Y.-Q. Guo, and Q. Yuan, *arXiv e-prints* (2019), 1905.12505.
- [58] D. Karmanov, I. Kovalev, I. Kudryashov, A. Kurganov, V. Latonov, A. Panov, D. Podorozhnyy, and A. Turundaevskiy,

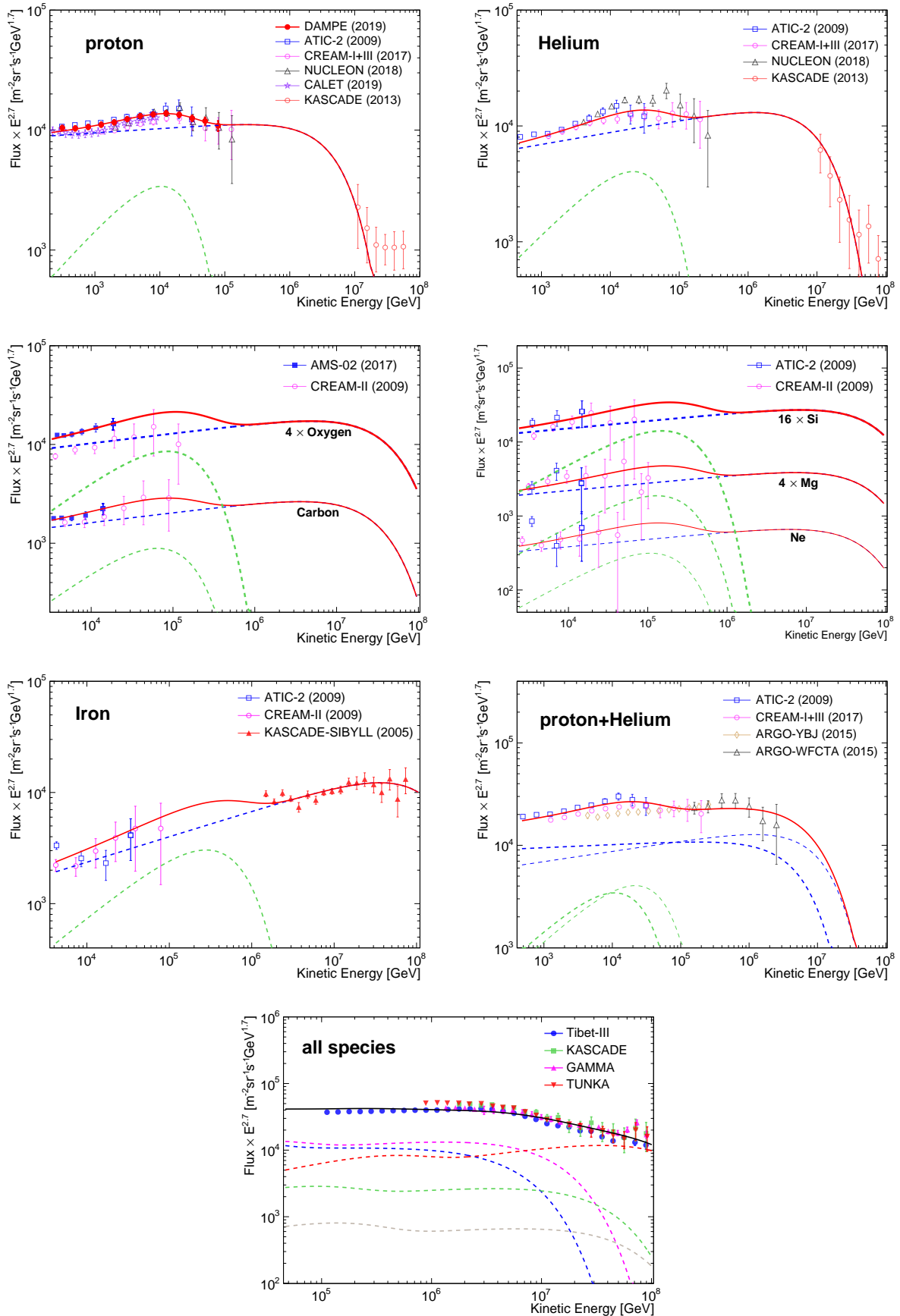


FIG. 3: Same as Fig. 2 but for model B.

- arXiv e-prints arXiv:1907.05987 (2019), 1907.05987.
- [59] Y. S. Yoon, et al., *Astrophys. J.* **728**, 122 (2011), 1102.2575.
- [60] P. Lipari and S. Vernetto, arXiv e-prints arXiv:1911.01311 (2019), 1911.01311.
- [61] H. S. Ahn, et al., *Astrophys. J.* **707**, 593 (2009), 0911.1889.
- [62] M. Aglietta, et al., *Astrophys. J.* **470**, 501 (1996).
- [63] M. Amenomori, et al., *Science* **314**, 439 (2006), astro-ph/0610671.
- [64] M. Aglietta, et al., *Astrophys. J. Lett.* **692**, L130 (2009), 0901.2740.
- [65] M. G. Aartsen, et al., *Astrophys. J.* **826**, 220 (2016), 1603.01227.
- [66] M. Amenomori, et al., *Astrophys. J.* **836**, 153 (2017), 1701.07144.
- [67] X. Bai, et al., arXiv e-prints (2019), 1905.02773.
- [68] S. N. Zhang, et al., in *Proc. SPIE* (2014), vol. 9144, p. 91440X, 1407.4866.